Design and Selection Criteria of Main Parachute for Re-entry Space Payload

Mahendra Pratap#,*, A.K. Agrawal@, and Swadesh Kumar#

#DRDO-Aerial Delivery Research & Development Establishment, Agra - 282 001, India
@Department of Mechanical Engineering, Indian Institute of Technology (BHU) Varanasi - 221 005, India
*E-mail: mahendra.pratap@adrde.drdo.in

ABSTRACT

Parachutes are used as a decelerator in the re-entry, descent, and landing of space recovery payloads, providing stability and desired descent rate for a safe landing. The selection of the main parachute is the most critical and important part of the space module recovery system. Parachute size is restricted by the required landing speed, materials, and weight of the payload. Parachute materials are selected based on the various forces experienced by the parachute. An investigation has been carried out to design a parachute system which gives less impact velocity, less angle of oscillation and less impact load for the landing of a crew module. Therefore, in this paper, selection criteria for the main parachute have been discussed considering recovery of re-entry space payload of 500 kg (unmanned) and 3500 kg (manned) class. Based on analysis carried out on the parachute size, canopy filling time, velocity reduction, peak deceleration, and opening shock, authors have proposed a unique type of solid canopy with slots (slots of the minimum area equivalent to geometry porosity) for the main parachute rather than a complex ringsail or disk-band type canopy. With this new concept, the parachute has been designed, developed and qualified through testing, trials and maiden flight of space capsule in LEO and is propose to use in the next manned space mission program.

Keywords: Drag force; Coefficient of drag; Filling time; Flight-path angle; Ringsail; Flat circular slotted canopy

NOMENCLATURE

S_o	Parachute surface area (m²)
S_{rm}	Frontal area of re-entry module (m²)
C_D	Drag coefficient
C_{Do}	Normal drag coefficient of parachute
C_{Drm}	Drag coefficient of re-entry module
D_o	Nominal diameter (m)
F	Drag force (N)
g	Gravitational constant (m/s²)
m	Total recovery mass (kg)
n	Parachute filling index
t	Time (s)
t_f	Canopy filling time (s)
V	Velocity (m/s)
V_0	Parachute velocity at line stretch (m/s)
T	Temperature (°C)
q	Dynamic pressure (kg/m/s²)
h	Altitude (m)
x	Horizontal axis in local coordinate system
β	Power of filling function
γ	Flight-path angle (degree)
ρ	Atmospheric density (kg/m³)
0	Nominal
t	Instant of time
p	Parachute
rm	Re-entry module
C_{Drm}	Coefficient of drag of re-entry module
LEO	Low earth orbit

1. INTRODUCTION

Parachute is an aerodynamic decelerator made of textile materials intended to retard and stabilise the payload during flight under the most critical conditions anticipated. Aerodynamic decelerators are used in many manned and unmanned space payload recovery experiments because of lighter weight, high strength to weight ratio, cost-effectiveness and high-performance reliability. Space Recovery Experiment (SRE, India), Apollo (USA), SOYUZ (Russia), Shenzhou (China) are some of the few examples where parachutes have been successfully used for crew module landing on earth. In any human space program, the recovery system invariably consists of two to three stage of parachutes i.e. pilot, drogue and main parachutes. A drogue parachute is essential for initial deceleration and stabilisation of module to reduce its velocity for the safe initiation of final recovery by large size parachute called as main parachute, which is inflated at predefined speed and altitude. To fulfill the requirements of the main parachute selection criterion, several types of parachute have been investigated worldwide and a comparative analysis has been presented in this paper.

In literature, it is found that the Apollo[1-2] parachute landing system was the most advanced, thoroughly engineered and rigorously tested system. The parachute system stabilizes and decelerates the crew carrying Apollo command module (5.9 ton payload) after the mission is completed to a descent velocity suitable for a water landing. In this program, two-stage reefed and a cluster of three ringsail parachutes having size of

25.45 m was used. The selection of parachute for Apollo was done after successful performance perceived in Mercury and Gemini landing systems. The Gemini[3-4] landing system uses a 25.85 m canopy diameter ringsail parachute for terminal descent. The Chinese Shenzhou[5] manned spacecraft resembled the Russian Soyuz[6] spacecraft but Shenzhou parachute was larger in size and all-new construction. The Shenzhou capsule employed the same landing technique as Soyuz. The single drogue, followed by single main parachute of, ringsail type, with area of 1200 sqm was used. Rives[7] has shown experimental results for the recovery of Apollo type re-entry payload (2800 kg) using a cluster of three tri-conical parachutes (22.9 m) as the main decelerator. In many planetary exploration missions, conical ribbon and disk-gap-band parachutes were frequently used due to low opening shock, quick opening and stability in terms of oscillation, as few are listed in Table 1[8]. It is clear from Table 1 that flat circular slotted canopy (henceforth circular slotted canopy) and aero-conical circular slotted canopy have not been used as the main parachute for a space mission. Therefore, this paper discusses and proposes the unique solid canopy with slot for the manned space mission.

Table 1.   Worldwide parachutes used in planetary exploration missions

Mission	Destination	Main parachute
Viking	Mars	16.2 m Disk Gap Band
Pioneer venus	Venus	4.94 m Conical Ribbon
Galileo	Jupiter	3.8 m Conical Ribbon
Mars pathfinder	Mars	12.7 m Disk Gap Band
MER	Mars	14.1 m Disk Gap Band
Cassini-Huygens	Saturn/ Titan	8.3 m Disk Gap Band

Mohaghegh[9] has shown that the filling time is a major criterion to classify the parachute types. In manned space missions, the space capsule recovery is required to be proven for both normal and launch pad abort situations. A quick filling of the canopy provides minimum loss of altitude during the inflation of the parachute. The peak deceleration due to rapid inflation is also one of the major criteria for the selection of main parachute. The maximum g-level during deceleration should be as low as possible within the human tolerance limit[10]. At a higher dynamic pressure, the ribbon or slotted type parachutes are used to avoid instability of payload whereas, at lower dynamic pressure, the scope of shape optimisation (smaller size or reefed parachute) is possible. When the capsule is decelerated to an equilibrium condition, the final parachute is deployed to retard the module for landing. In general, the preferred maximum velocity for final (main) parachute deployment in manned space mission, worldwide is 80 m/s at 3 km altitude[1,3,5,6] to reduce opening shock, save weight, material strength. The same parameters were used in design of SRE and HSP. Both the recovery systems were launched in maiden space flights for qualification tests. The authors have also chosen the same parachute deployment conditions for the design of the main parachute for the proposed man mission program.

For Indian first space payload recovery mission, SRE[11] unmanned re-entry payload (500 kg) was designed and tested in LEO for microgravity study using the aero-conical parachute as shown in Fig. 1(a). It consists of two-stage parachutes, one drogue and one main parachute (aero-conical, size 12.44 m) without any redundancy and forced inflation floatation system to afloat the capsule over the sea. After the success of SRE, the study for human space programme (HSP) was initiated with payload mass of 3500 kg. In this system, a cluster of two parachutes (one as redundant) with one stage was reefed investigated for final recovery decelerator. The final configuration of this parachute is as shown in Fig. 1(b). All essential qualification tests were carried out including one maiden space flight and followed by pad abort test.
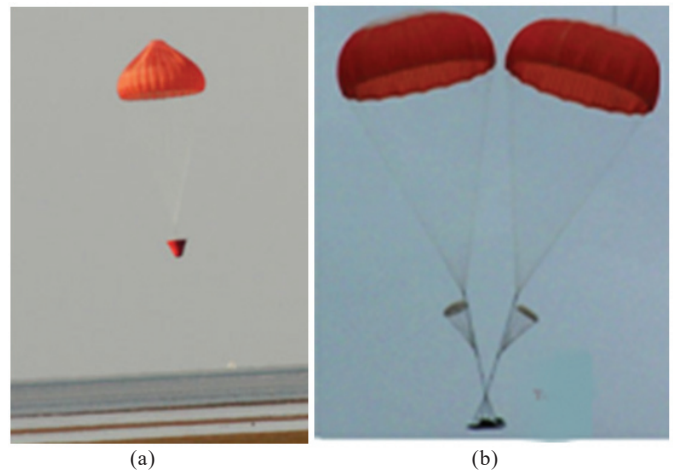

(a)   (b)

Figure 1.   (a) Aero-conical parachute used in SRE. (b) circular slotted parachute for HSP.

2.   MATHEMATICAL MODEL

For a parachute deployed in air, the time interval, from the instant of canopy and lines stretched to the point when the canopy is first fully inflated is known as parachute filling time[12]. If parachute size is very large like HSP (35.20 m diameter), it is likely to be heavy and bulky, therefore, inflation is controlled by inserting the reefing line at the skirt of a parachute and thereby limiting the parachute opening force to a preselected value. To understand the effect of various parameters on the selection of a parachute, a point-mass trajectory is simulated. A mathematical model for calculating the flight dynamics of the parachute has been described by Gamble[13]. In this paper, 2-degree of freedom mathematical modelling is carried out assuming parachute-payload as one body, each one with its own position, velocity, orientation, and angular velocity vectors.

2.1 Basic Equilibrium Equations

The study of parachute deployment requires the numerical solution to the equations of motion. It is described by a simplifying the mathematical model. Following assumptions are made for formulating the mathematical equations:
- 'm' and 'g' are constant
- No wind condition prevails
- Flight path angle(γ) is negative

- Re-entry payload is stable and steady-state during the main parachute deployment.
- The forces are assumed to act along the airspeed direction which is also assumed to be the direction of deceleration.

Basic equilibrium equations for parachute-body mass are as given in Eqn. (1) to Eqn. (3) are,

$$F_p + F_{rm} = q(C_{D0}S_0 + C_{rm}S_{rm})$$ (1)

$$q = \frac{1}{2}\rho V^2$$ (2)

$$F_p + F_{rm} = mg$$ (3)

Atmospheric density changes with altitude, given as

$$\rho = f(h)$$ (4)

The variation of air density with altitude is taken as per ISA conditions.

2.2 Point Mass Trajectory Model

A point mass trajectory is developed considering the parachute payload which is moving at a flight path angle (γ) < 0. Figure 2 shows a simplified free-body diagram of forces involved in parachute deceleration. The free body diagram is used to generate equation within a boundary:

During vertical descent of parachute, the equations of motion, Newton 2nd Law, written as Eqns. (5)-(8) are,

$$\frac{dV}{dt} = -g\sin\gamma - \frac{F_p}{m}$$ (5)

$$\frac{d\gamma}{dt} = -\frac{g\cos\gamma}{V}$$ (6)

Kinematics relations

$$\frac{dh}{dt} = +V\sin\gamma$$ (7)

$$\frac{dx}{dt} = V\cos\gamma$$ (8)

The instantaneous drag force generated by the parachute during flight is varying as proportional to the square of the velocity and function of time, as given by Eqn. (9).

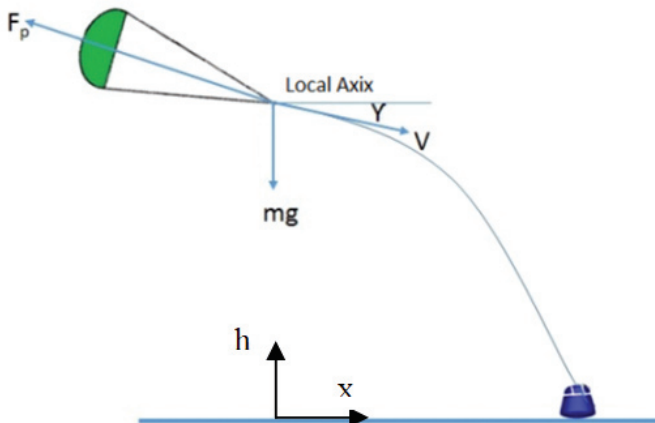$$F_p = \frac{1}{2}\rho_{altitude}V^2(t)C_DS(t)$$ (9)

Figure 2. Flight path trajectory of re-entry module.

3. CRITERIA FOR SELECTION OF MAIN PARACHUTE

Various types of parachute have been investigated considering payload masses of 500 kg and 3500 kg to determine the best configuration as basis of selection criteria. The final selection is based on drag area variation, filling time, opening shock and peak deceleration.

3.1 Drag Area Variation

Canopy inflation involves dynamic and non-linear process, which is very difficult to simulate exactly. The canopy expansion during inflation is resisted by the structural tension of parachute until the full inflation occurs. The parachute inflation can be described by matching drag area growth $(C_DS)_p$. The drag area variation is assumed to be a second-order function of time for solid textile canopies and a linear function of time for slotted canopies[14]. Therefore, for all the parachutes, the instant area growth during inflation for unreefed parachute can be written as,

$$C_DS(t) = (C_DS)_0\left(\frac{t}{t_f}\right)^\beta$$ (10)

where β = 1 for slotted canopy parachute, and
β = 6 for solid canopy parachute

The drag area variation with respect to time, written as in Eqn. (10) has been modelled and analysis has been carried out in MATLAB. This is input for further analysis and selection of main parachute. The drag area variation increases for slotted canopy faster than solid canopy as shown in Fig. 3.

3.2 Canopy Filling Time

Generally, the main parachute stage takes a large time to develop; therefore, one stage reefing is inserted at the skirt of a parachute to control the behaviour of inflation. To solve all the above equations, following assumptions and input data are considered as per the specification of space mission requirements:

(i) Maximum velocity for main parachute deployment (V_0) kept as 80 m/s, in view of control of the opening shock, limitation in materials and for maintaining the system reliability.

(ii) Altitude (h) as 3 km (density = 0.9104 kg/m³), is commonly selected altitude for main parachute deployments to avoid high canopy loading and bulky shape.

(iii) Γ = -16°, is assumed angle for representation as, during main parachute deployment, the re-entry payload may not
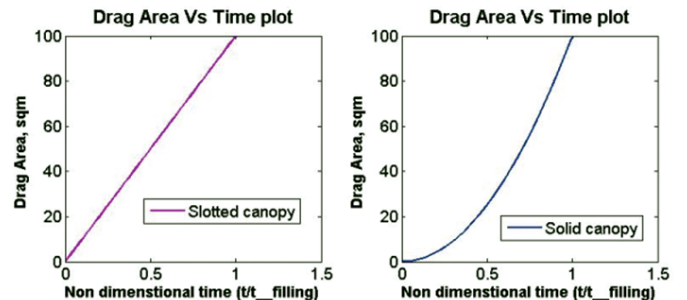

Figure 3. Drag area variation for slotted and solid canopy.

be falling vertically in all possible scenarios.

(iv) $V_{terminal}$ = 8 m/s is safe terminal speed for water landing of re-entry payload.

The available of literature shows that the coefficient of drag and filling time index depend on the shape of the canopy. Ludtke[15] has described the drag coefficient and filling time index (n) for general parachute opening force analysis. Based on the above inputs and empirical relation (filling time = nD_o/V_o), the canopy filling time of various parachutes is estimated for the same drag area (100 m²) and deployment condition and is as shown in Fig. 4.

Figure 4 shows that for the same drag area, even being a slotted canopy, ringsail parachute is the fastest opening parachute due to its construction and design. The other solid canopies like tri-conical and aero-conical are also having less filling time than ribbon and disk band gap parachutes and at par with ringsail. Therefore, a solid canopy with linear slots has quick opening characteristics.
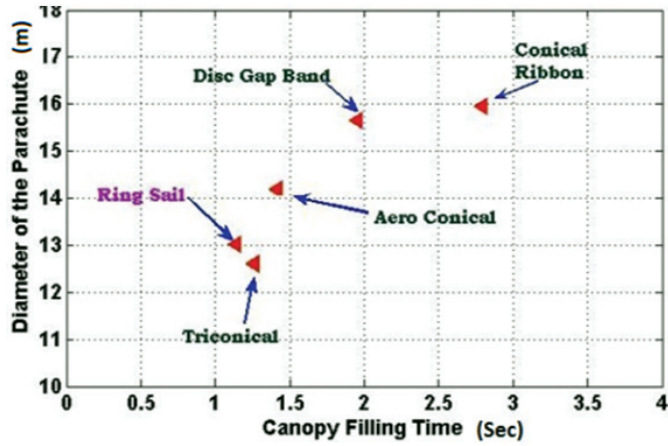

Figure 4. Diameter vs filling time of various parachutes.

3.3 Parachute Sizing and Shape

The required surface area (S_o) of the parachute is found by rearranging the drag force equation in Eqn. (1). One can find the nominal area of the parachute (as payload drag area is negligible compared to a parachute) from in Eqn. (11),

$$S_0 = \frac{mg}{q_{terminal} \ C_{D0}} \qquad (11)$$

The size estimation for 500 kg and 3500 kg payload class is carried out for various parachutes as shown in Table 2. It is clear that ringsail and circular slotted parachute has a minimum size and, hence less canopy mass which is desirable for any space mission.

3.4 Angle of Oscillation

The angle of oscillation is a critical requirement for crew module for a safe descent. Wind tunnel data has been plotted by Cruz[16] for the angle of oscillation vs the drag coefficient. Knacke[17], et al. (from experimental data on the angle of oscillation) are used for (6) ±15° is less than that for solid canopy (±20°). However, in the cluster, (the configuration of a solid canopy), oscillation is absorbed by the canopy interfacing.

Table 2. Estimated size of parachutes for 500 kg and 3500 kg payloads

Parachute type	C_{Do} (selected coefficient of drag)	Size of parachute (m)	
		500 kg payload	3500 kg payload
Conical ribbon	0.50	17.84	47.22
Ring sail	0.75	14.57	38.55
Disc gap band	0.52	17.5	46.3
Aero-conical	0.635	15.83	41.89
Tri-conical	0.80	14.11	37.33
Circular slotted	0.75	-	35.20

Therefore, solid canopy with minor slots has been selected for the experimental investigation to determine its suitability for a space mission in the cluster configuration.

3.5 Parachute Opening Shock Load

Selection of parachute materials is decided based on the maximum opening load that a parachute may experience during flight. In design analysis for parachute, opening load for various types of parachute considering 500 kg and 3500 kg payload, is calculated using the trajectory method and plotted in Figs. 5 and 6, respectively. The maximum opening load occurs in ringsail parachute, whereas in other parachutes, it is lesser and comparable. The effect of payload mass can be seen in tri-conical, disc gap band, aero-conical and conical ribbon. For 500 kg payload, the opening load of a tri-conical, circular slotted and aero-conical parachute is lower than that for ringsail parachute. When the payload mass is increased to 3500 kg, the opening loads of tri-conical, disc gap band, aero conical, circular slotted and conical ribbon are also lower than ringsail. Therefore, the circular slotted parachute has a lower opening shock than ringsail and is thus suitable for man mission.

From Eqns. (1) to (9), analysis for velocity reduction with time has been carried out in MATLAB considering payloads
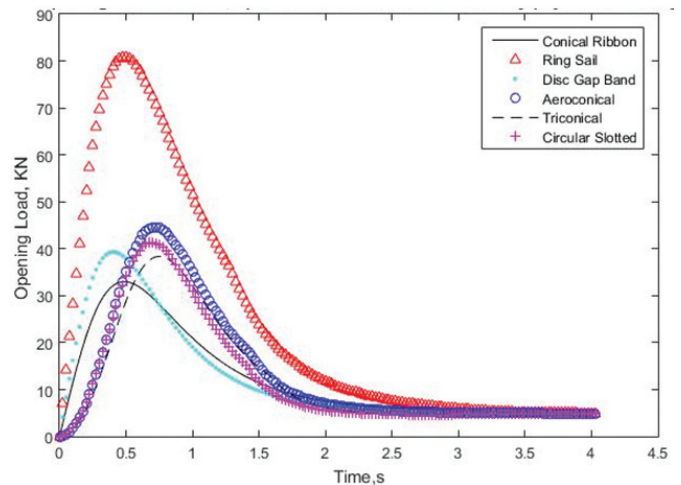

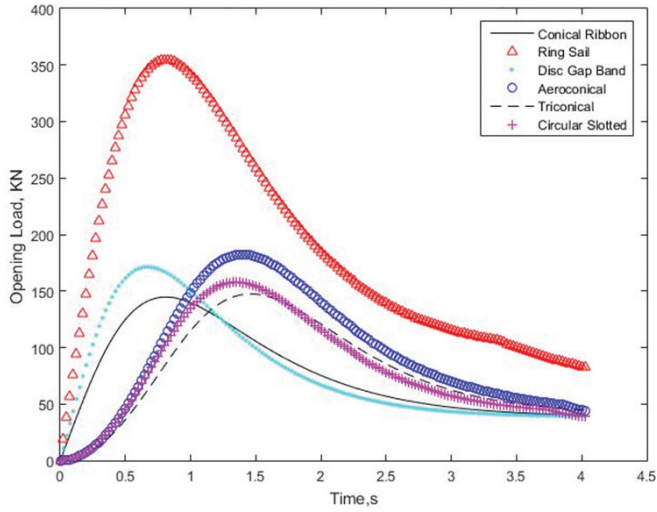Figure 5. Opening load variation of different parachutes for 500 kg payload.

Figure 6. Opening load variation of different parachutes for 3500 kg payload.

as 500 kg and 3500 kg, and is represented in Figs. 7 and 8, respectively. The decreasing trend of the velocity of a payload is due to the inflation characteristics of the individual parachutes. Ringsail parachute reaches terminal velocity much faster than other parachutes due to lesser inflation time. However, velocity reduction in the circular slotted canopy is initially slow but later on faster.

3.6 Peak Deceleration

Peak deceleration is a key parameter for crew-carrying module in which the *g*-level is limited as per the survival requirements of the crew members. Acceleration analysis of various parachutes for 500 kg and 3500 kg payloads are estimated and as shown in Figs. 9 and 10, respectively. The peak deceleration (in terms of *g* value) for ringsail parachute is much higher compared to the same for other parachutes. From the analysis, it is found that the circular slotted parachute has less *g* value than that for ringsail.
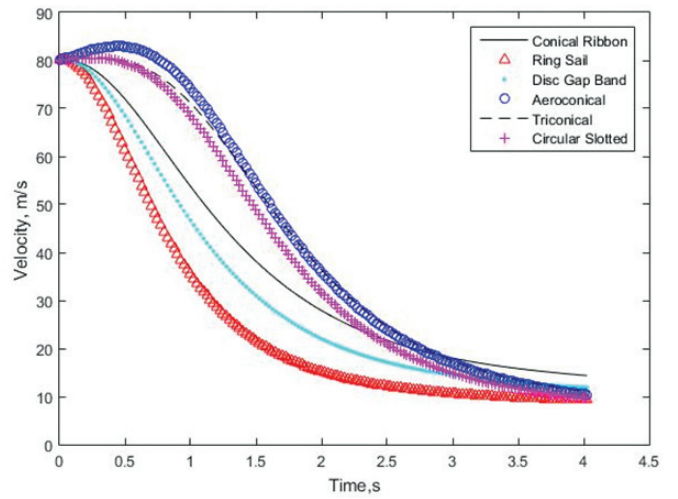

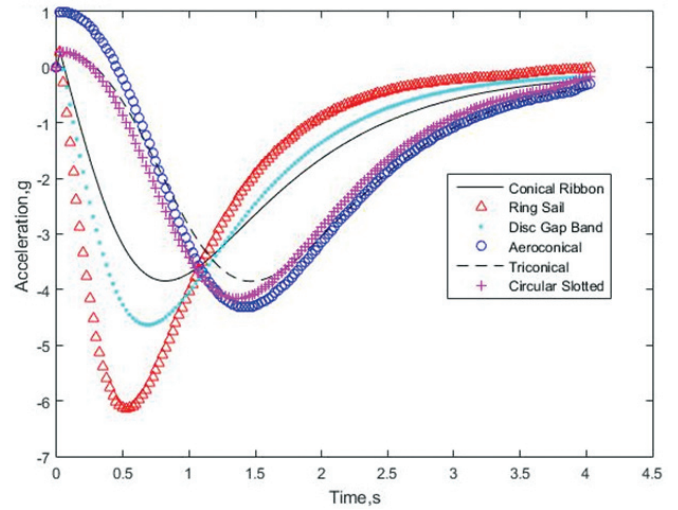**Figure 8. Velocity reduction of different parachutes for 3500 kg payload.**

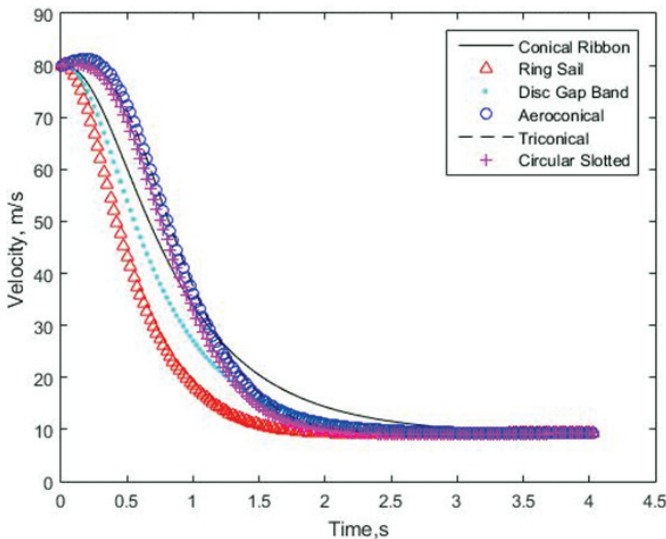**Figure 9. Deceleration of different parachutes for 500 kg payload.**

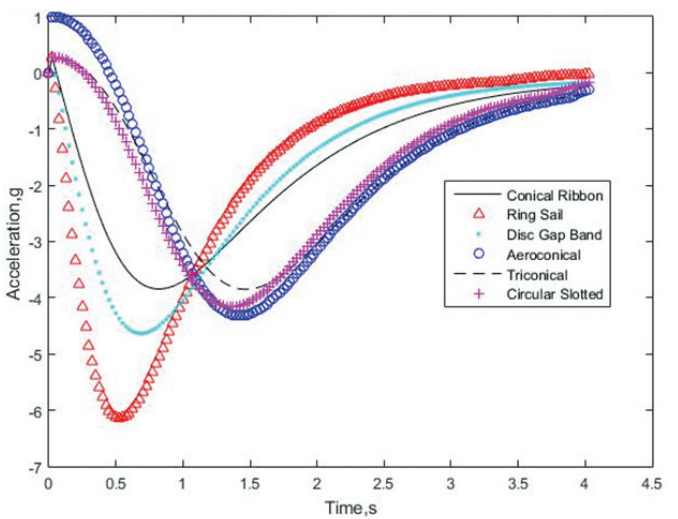**Figure 7. Velocity reduction of different parachutes for 500 kg payload.**

Figure 10. Deceleration of different parachutes for 3500 kg payload.

4. PROPOSED PARACHUTE CONFIGURATION

To fabricate a stable parachute, it is necessary to have geometry porosity and good permeability of materials. From this study, it is found that parachute with less oscillation and quick opening characteristics is suitable for the safe landing of the space module. Therefore, to increase the stability of the solid canopy parachute, slots of minimum area (equivalent to geometry porosity) are distributed either circumferential or radial or combined in gores. Other parameters like peak opening load and acceleration (g-level) of parachutes can be controlled by introducing reefing. The circumferential slots have been made in such a way that the reverse flow field from the slots would generate additional drag similar to the ringsail parachute. In a typical gore pattern in which the base of the upper gore is made wider than the top of the lower gore, the expected flow field generated with this arrangement is as shown in Fig. 11.
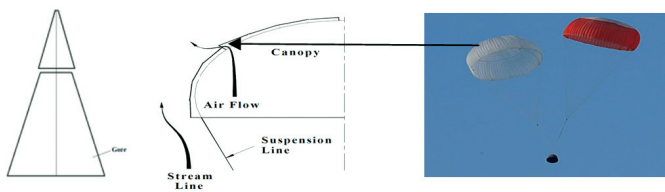

Figure 11. Gore layout and flow field in steady descent in solid slotted parachute.

5. CONCLUSIONS

The prime purpose of this study is to design such a parachute which gives maximum drag force, minimum flow disturbance, and provides steady descent to the crew module. The mathematical analyses and experimental investigation show that the circular slotted parachute has less opening shock in reefed condition and also the minimum size for the same payload amongst the various parachutes. Circular slotted parachute is easy to manufacture whereas ringsail requires high skill to maintain the sail dimension, band-gap, and porosity of the overall parachute. One of the outcomes of the experimental investigation is the parachute coefficient of drag, which is measured and compared with the value found in literature. It is found to be at par with ringsail as reported in Table 3. This investigation is carried out in the subsonic application to validate the proposed design parameters. The result of the above analysis and experimental testing in dynamic and simulated flights indicate that this configuration of parachute gives stable and steady descent to the crew module.

Table 3. Coefficient of drag of selected main parachute for space mission

Parachute type	Nominal C_d, (Literatures)	Av. C_d from wind tunnel testing	C_d from air drop test	C_d taken for design
Circular slotted	0.75 - 0.8	0.73	0.69-0.83	0.75 ± 10%

Conflict of Interest: None

REFERENCES

1. Knacke, T.W. The Apollo parachute landing system. AIAA aerodynamic decelerator system conference, EI Centro, Calif., 1968; USAF report No. FTC-TR-69-11.
2. Mickey, F.E.; McEwen, A. J.; Ewing, E. G.; Huyler, E.C. & Khajeb-Nouri, B. Investigation of prediction method for the loads and stresses of Apollo type spacecraft parachutes, 1970; Volume-I, report No. NVR-6431, Northrop Corp., Ventura division.
3. John, Vincze. Gemini spacecraft parachute landing system, 1966; NASA report No. TN D-3496, pp. 6.
4. Henry, A. Lee; Peter, J. Costigan & James, S. Bowman, Jr. Dynamic model investigation of a 1/20-scale Gemini spacecraft in the Langley spin tunnel, 964; NASA technical note NASA-TN-D-2191.
5. Guo, Zhi Mei1.; Miao, Qi Long.; Wang, Shu Dong & Huang, Li. Prediction of the trajectory of the manned spacecraft Shenzhou-7 deploying a parachute based on a fine wind field. *Sci. China Earth Sci.,* 2011, **54**(9), 1413–1429.
   doi: 10.1007/s11430-011-4234-x.
6. Soyuz Spacecraft. https://en.wikipedia.org/wiki/Soyuz. (Accessed on 16.04.19).
7. Rives, J.; Portigliotti, S. & Leveugle, T. Atmospheric re-entry demonstrator descent and recovery sub-system qualification test - flight dynamics and trajectory modeling during descent. *In* 14th AIAA aerodynamic decelerator systems technology conference and seminar 2011. Published online 2012.
   doi: 10.2514/6.1997-1441.
8. Steve, Lingard. Parachute system technology short course on aerodynamics 1 & 2 (unsteady), Heinrich Parachute Technology, 2008; YUMA Arizona USA.
9. Mohaghegh, F. Parachute filling time: a criterion to classify parachute types. *In* Proceeding of 19th AIAA aerodynamic decelerator systems technology conference and seminar, 2007. Session: ADS-17: Design and Development VII. Published Online: 2012.
   doi: 10.2514/6.2007-2527.
10. Lowry, Charles. Man-rating the Apollo and other earth landing systems. *In* 21st AIAA aerodynamic decelerator systems technology conference and seminar, 2011.
    doi: 10.2514/6.2011-2559.
11. Sidana, M.L.; Jain, J.C.; Pal, A. & Goel, Ankur. Design, development, and validation of a recovery system for a 500 kg re-entry payload. *In* 18th AIAA aerodynamic decelerator systems technology conference and seminar 2005, AIAA 2005-1638. Session ADS-10: Atmospheric Re-entry, 2005.
    doi: 10.2514/6.2005-1638.
12. Knacke, T. W. Parachute recovery systems design manual. NWC TP 6575, Para publishing, Santa Barbara, California, 1992. ISBN 0-915516-85-3.
13. Joe D., Gamble. A mathematical model for calculating the flight dynamics of a general parachute-payload system. NASA report No. NASA-TN-D-4859, 1968.
14. Macha, J.M. A simple, approximate model for parachute inflation. *In* Aerospace design conference, 1993.

doi: 10.2514/6.1993-1206.

15. Ludtke, W.P. Notes on a generic parachute opening force analysis. *In* Proceeding of 9th AIAA aerodynamic decelerator systems technology conference and seminar, 1986.

16. Juan, R. Cruz. Flight mechanics-I, trajectory analysis, Heinrich Parachute Technology Short Course. 2008, YUMA Arizona USA. Juan.R.Cruz@NASA.gov; 757-864-3173.

17. Ewing, E.G.; Bixby, H.W. & Knacke T.W. Recovery system design guide. 1978. Report No. AFFDL-TR-78-151.

ACKNOWLEDGMENTS

CONTRIBUTORS

Mr Mahendra Pratap has acquired his BE (Mech, Hons) from Moti Lal Nehru Regional Engineering College, Allahabad, in 1989 and MTech (IM) from IT BHU Varanasi, in 2008. Presently working as a Group Director (Para) at DRDO-Aerial Delivery Research & Development Establishment, Agra. The author also has worked in the field of reliability and quality assurance division. He has published 17 papers in seminars and conferences. He has been awarded Lab young scientist and Group Technology awards.
In the current study, he has designed the parachute system and also carried out the testing, packed life analysis as per space standard requirements. He has generated mathematical model and various testing using the solid canopy as the main decelerator and proposed configuration of canopy for better stability and drag coefficient.

Professor A K. Agrawal has obtained his BE (Mechanical Engineering) from MNREC Allahabad, in 1979, MTech and PhD from IIT Kanpur. At present, he is a Professor in the Department of Mechanical Engineering IIT(BHU) Varanasi India. His area of interest is reliability, quality control, mathematical modeling and simulation, six sigma, optimisation, industrial engineering. He has credits of many national and international papers.
In current the study, he has extended logistic support and overall guidance to formulate the mathematical equations and comparative analysis on parachute inflation time. He has also contributed to a literature survey on the related topics and reviewed the paper.

Mr Swadesh Kumar has obtained his MTech from IIT Kharagpur, India in the field of CFD analysis. At present, he is working as a scientist in parachute division, DRDO-Aerial Delivery Research & Development Establishment, Agra. He has designed various parachutes for unmanned aircrafts, recovery payloads etc. He has published many papers in seminars and conferences.
In the current study, he was associated in design, testing and fabrication of parachutes of 3500 kg re-entry payload. He has developed MATLAB program and simulated the various design parameters.